Spring 2018

Connecting the Dots: A New Method to Determine Radiation Yield during Electron Beam (EB) Polymerization Reactions via Raman Spectroscopy

Renae Kurpius
University of Iowa

CONNECTING THE DOTS: A NEW METHOD TO DETERMINE RADIATION YIELD DURING ELECTRON BEAM (EB) POLYMERIZATION REACTIONS VIA RAMAN SPECTROSCOPY

by

Renae Kurpius

A thesis submitted in partial fulfillment of the requirements
for graduation with Honors in the Chemical Engineering

_____

Julie Jessop
Thesis Mentor

Spring 2018

All requirements for graduation with Honors in the
Chemical Engineering have been completed.

_____

David Rethwisch
Chemical Engineering Honors Advisor

Connecting the Dots: A New Method to Determine Radiation Yield during Electron Beam (EB) Polymerization Reactions via Raman Spectroscopy

by

Renae E. Kurpius

A thesis submitted in partial fulfillment of the requirements
for graduation with Honors in Chemical Engineering

_____
Julie Jessop
Thesis Mentor

May 2018

All requirements for graduation with Honors in
Chemical Engineering have been completed.

_____
David Rethwisch
Chemical Engineering Honors Advisor

Abstract

Electron-beam (EB) polymerization is a fast, solvent-free, low-energy means of polymerizing inks, thin films, and coatings such as those used in food packaging. During EB polymerization, accelerated electrons interact with liquid monomer molecules to form radicals, which continue to react with other monomer molecules and form long chain, solid polymers. The final polymer properties are dependent on the monomer chemistry, as well as processing conditions such as dose (i.e., the amount of energy that is absorbed by the sample), belt speed (i.e., the rate at which the sample travels through the electron-beam unit), and dose rate (i.e., the rate at which energy is delivered to the system). Unfortunately, the relationships among formulation chemistry, processing conditions, and final polymer properties are not well understood, thereby limiting the growth of EB polymerization in industry. One reason these relationships are not well characterized is the unpredictable nature of radical formation during EB polymerization. Determination of apparent radiation yield (i.e., number of measurable radicals created per 100 eV of energy absorbed by the system) can facilitate understanding of how radicals are formed during EB reactions, which will fill in the knowledge gaps and allow for better prediction of final polymer properties. Limited research has been conducted to determine the apparent radiation yield of EB-cured polymers, and the work that has been done relies on multiple assumptions. The goal of this research project was to develop a method for determining the apparent radiation yield.

Apparent radiation yield is proportional to the apparent rate of initiation (i.e., the change in radical concentration with respect to time). The radical concentration could not be measured directly because the concentration of radicals in the system is so small and because radicals are not easily detected with spectroscopy or other analytical techniques. Instead, a highly reactive

inhibitor molecule was added to the formulation, which reacted with the radicals formed by the EB. Each inhibitor molecule reacts with one radical, thus the concentration of radicals is equal to the concentration of inhibitor. Raman Spectroscopy was used to find the delay in conversion caused by the added inhibitor. The inhibitor concentration was plotted versus that conversion delay, and the slope of the resulting best-fit line was the apparent rate of radical formation, which was used to calculate the apparent radiation yield. Using this method, the apparent radiation yield of benzyl acrylate was determined to be 60±40, which is consistent with the theoretical number of radicals that could be produced by 100 eV of energy.

Table of Contents

Table of Figures

Table of Tables

Introduction

Electron-beam (EB) polymerization has many benefits over thermal and photo-polymerization. It is a fast, solvent-free, low-energy means of polymerizing inks, thin films, and coatings such as those used in the food packaging and medical devices industries. Initiators, which can migrate out of the packaging, are not required to begin the reaction, making this technology well-suited for use in food packaging and medical industries where contaminants are heavily regulated by governmental agencies. Unlike photopolymerization, EB polymerization can cure thick and pigmented samples because accelerated electrons are not hindered by pigments, fillers, and thick depths. Benefits over thermal polymerization include better spatial and temporal control, allowing for more targeted polymerization of samples.

Despite these advantages, use of EB polymerization is limited due to lack of fundamental understanding of the curing process. The final properties of the polymers created during EB polymerizations are dependent on the monomer chemistry, as well as processing conditions such as dose (i.e., the amount of energy that is absorbed by the sample), belt speed (i.e., the rate at which the sample travels through the electron beam unit), and dose rate (i.e., the rate at which energy is delivered to the system). Unfortunately, the relationships among formulation chemistry, processing conditions, and final polymer properties are not well understood.

One reason these relationships are poorly characterized is the unpredictable nature of radical formation during EB polymerization. EB polymerization cannot be monitored in real time, as the reactions occur too quickly, and the accelerated electrons create a harsh environment, which would damage equipment used for real-time reaction monitoring. These issues make characterization of the reactions difficult. Furthermore, EB initiation is a complex

process. Once a radical forms, it can go on to react with a monomer, creating an activated monomer, which can then propagate and form a long chain polymer. Radicals can also form along a polymer chain and then interact with a radical from a nearby polymer chain, forming a cross-link. These are just a few examples of the many complex reactions that can take place after radical formation.

Radiation yield, G_R, is defined as the number of primary radicals created per 100 eV of energy absorbed by the system (Chapiro, 1962). This property can facilitate understanding of how radicals are formed during EB reactions. Radiation yield is described using Equation 1:

$$R_R = G_R \rho \frac{dD}{dt} \quad (1)$$

where R_R is the rate of radical formation, ρ is the density, and dD/dt is the dose rate to which the system is exposed.

Limited studies have been conducted to determine the radiation yield in EB systems; however, they have several shortcomings. In one study, rate of initiation (R_i) was determined through derivation of the kinetic scheme and was then used to calculate G_R values. However, this method relies on assumptions such as initiation takes place randomly in the sol and gel phases, random polymerization takes place in the network swollen with monomer, no chain transfer, and termination is unimolecular, all of which may or may not be true (Labana, 1968). Other research has focused on calculating radiation yield for styrene and methyl methacrylate monomers; however, these studies frequently interchanged G_i, G_R, and G(-m) values, which are not explicitly defined, in their calculations without explanation (Squire, et al., 1972), (Allen, et al., 1974). Each of these values has a different technical definition, and therefore using these values

interchangeably is inaccurate. Careful definition of these terms would allow for more direct comparisons among G values.

In this study, a protocol using a free-radical inhibitor was developed to calculate the radiation yield in EB polymerizations. This method was adapted from a previous study focused on determination of radiation yield in gamma-initiated polymerizations (Chapiro, 1962). The dose rates used during gamma-irradiation are several orders of magnitude smaller than those used in EB polymerization. The total energy delivered by gamma-irradiation is also much lower than that delivered in EB systems. Due to these differences in the two initiation methods, the resulting radiation yields may not be comparable to one another. It is expected that the radiation yield values for monomers initiated with EB will be much larger than those initiated with gamma-rays because of the higher dose rates.

An important distinction must be made when adapting the inhibition method used in the 1962 Chapiro study for determination of radiation yield. As previously stated, G_R is the number of primary radicals that are created per 100 eV of energy. G_R encompasses all measurable radicals, as well as those that are non-reactive or otherwise inert (Equation 2):

$$G_R = G_R' + G_n \tag{2}$$

where G_R' is the apparent radiation yield (i.e., number of measurable radicals created by 100 eV of energy absorbed by the system) and G_n encompasses all non-reactive and otherwise inert species that cannot be measured using this inhibitor method. The reactivity of a species is dependent on how the bonds are broken. An excited-state monomer may cleave into two radicals, with one relatively stable radical and another that is reactive. Some radicals may also get trapped

and be unable to react. Both situations lead to radicals that will not react with the added inhibitor, and therefore, will not be counted by the experimental method.

Since the non-reactive species cannot be measured, the protocol developed in this study specifically determines the apparent radiation yield, G_R'. G_R' can be directly substituted into Equation 1, and the equation can be rearranged to solve for apparent radiation yield as follows:

$$G_R{}' = \frac{R_R{}'}{\rho \frac{dD}{dt}} \tag{3}$$

where $R_R{}'$ is the apparent rate of radical formation.

The goal of this research project was to develop a new method for determining radiation yield. Understanding how many radicals are formed and how many of them go on to initiate polymerization is the first step in building the relationship among monomer chemistry, processing conditions, and the final polymer properties. Determination of radiation yield will allow for development of a relationship between radical formation and final polymer properties, as well as help expand EB polymerization – both for use in its current fields and for use in new fields such as the automotive and architectural industries, where more advanced polymer properties are required.

Experimental

Materials

Benzyl acrylate (BA, TCI America) was the monomer used in this study. BA was chosen because acrylates are commonly used in industry, and it contains a phenyl ring, which is required to ensure reliable analysis using Raman spectroscopy (Schissel, Lapin, & Jessop, 2014). Hydroquinone (HQ, TCI America) was the free-radical inhibitor used in conjunction with BA to

obtain rate of initiation for this study. Both chemicals were used as received and are shown in Figure 1.

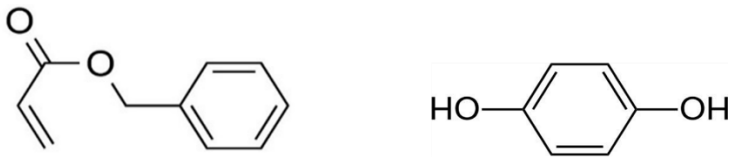

Figure 1. Structures of the monomer benzyl acrylate (left) and the inhibitor hydroquinone (right).

Methods

Sample Preparation

Formulations were prepared by varying the amount of HQ in BA: 0.0%, 0.25%, 0.5%, 1.0%, 1.5%, and 2.0% by weight HQ. Ten sets of Q-panels were prepared with six aluminum weigh boats attached to each panel. Each weigh boat on a panel contained one of the six formulations in the HQ concentration series. To create a 200 µm film, 63 µL of formulation was pipetted into a weigh boat. With a film thickness of 200 µm, it is a reasonable to assume full penetration of the accelerated electrons at a voltage of 200 kV.

Electron-beam Exposure

EB polymerization was used to cure the samples. The polymerization took place on an EBLab unit (Comet Technologies, Inc.). The voltage of the lab unit was set to 200 kV. Nitrogen gas was used to reduce the concentration of oxygen to below 200 ppm. A combination of 10 belt speeds and doses were used to maintain a constant dose rate of 197 kGy/s for each trial. Each Q-panel was exposed to a different combination of dose (ranging from 20-200 kGy) and belt speed (ranging from 3-30 m/min); specific combinations for each trial are given in Table 1.

Table 1. Dose and belt speed combinations for each trial

Dose (kGy)	20	22	25	29	33	40	50	67	100	200
Belt Speed (ft/min)	30	27	24	21	18	15	12	9	6	3

Raman Spectroscopy

Raman Spectroscopy was used to determine monomer conversion. After EB exposure, the samples were pipetted into quartz capillary tubes. Raman spectra of the samples (both formulations containing inhibitor and neat monomer) were collected using a holographic probe head (Mark II, Kaiser Optical Systems Inc.) via a 100 μm collection fiber. A single-mode excitation fiber carried an incident beam of 785 nm near-infrared laser to the quartz capillary tube. Laser power at the sample was approximately 180 mW. Spectra were collected with an exposure time of 250 ms and 5 accumulations. For each sample, 10 spectra were collected and averaged to provide accurate values to use when calculating monomer conversion.

Data analysis was completed using Holoreact software, Revision: 2.4.4, to gather peak height data for reaction and reference peaks of polymerized sample (P) and unreacted monomer (M). An example Raman spectrum is shown in Figure 2. The reference peak was measured at 1595-1618 cm^{-1} (indicative of the -C=C- bonds in the phenyl ring) and the reaction peak at 1623-1650 cm^{-1} (indicative of the -C=C- vinyl bond of the acrylate). The reference peak is needed to eliminate error caused by variations in the instrument. With this information, conversion, α, can be calculated (Equation 4):

$$\alpha = \left(1 - \frac{I_{rxn}(P)/I_{ref}(P)}{I_{rxn}(M)/I_{ref}(M)}\right) \times 100 \quad (4)$$

where $I_{rxn}(P)$ and $I_{ref}(P)$ are the peak intensities of the reaction and reference peak of the polymerized sample, respectively; $I_{rxn}(M)$ and $I_{ref}(M)$ are the peak intensities of the reaction and reference peak of the unreacted monomer, respectively (Schissel, Lapin, & Jessop, 2014).

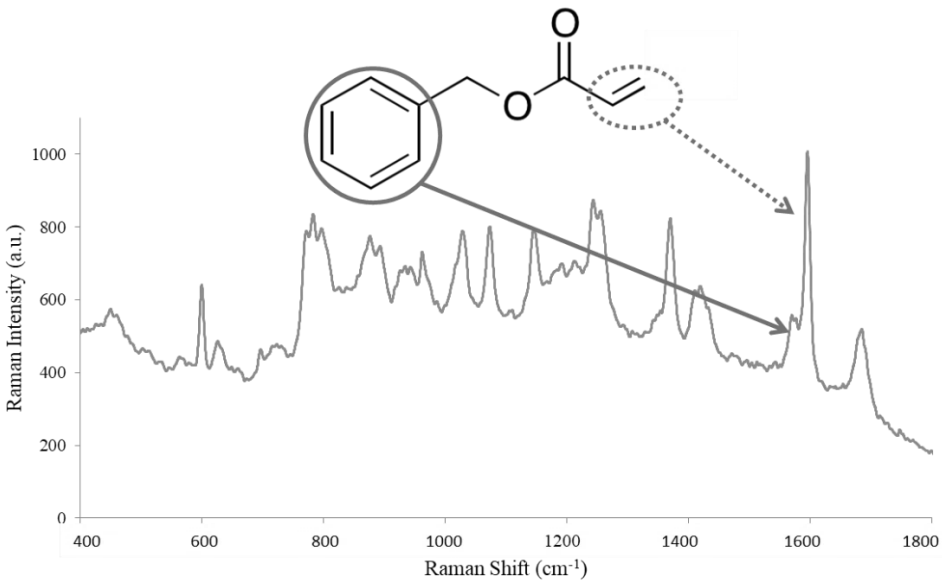

Figure 2: Representative Raman spectra used to calculate conversion. The portion of the chemical structure circled with the solid line represents the phenyl ring in the acrylate, and its representative peak at 1610 cm^{-1} remains at a constant height throughout the reaction. The portion of the structure circled with the dotted line refers to the double bond in the acrylate, and its representative peak at 1640 cm^{-1} decreases in height as the monomer is converted to polymer.

Results

A protocol was developed to determine apparent radiation yield for monomers undergoing free-radical polymerization via EB irradiation (see Figure 3). Formulations containing monomer and inhibitor were polymerized under the EB, and the conversion of monomer was calculated using Raman spectroscopy. With these conversion values, a kinetic profile was created to determine the conversion delay for each inhibitor concentration (see Figure 4 as an example). Time was calculated using the following equation:

$$t = \frac{Beam\ width\ (m)}{belt\ speed\ (m/min)} \tag{5}$$

where the beam width is a fixed, known value and belt speed is one of the known variables. The conversion delay is obtained by identifying the point at which all inhibitor is consumed and the conversion begins to increase.

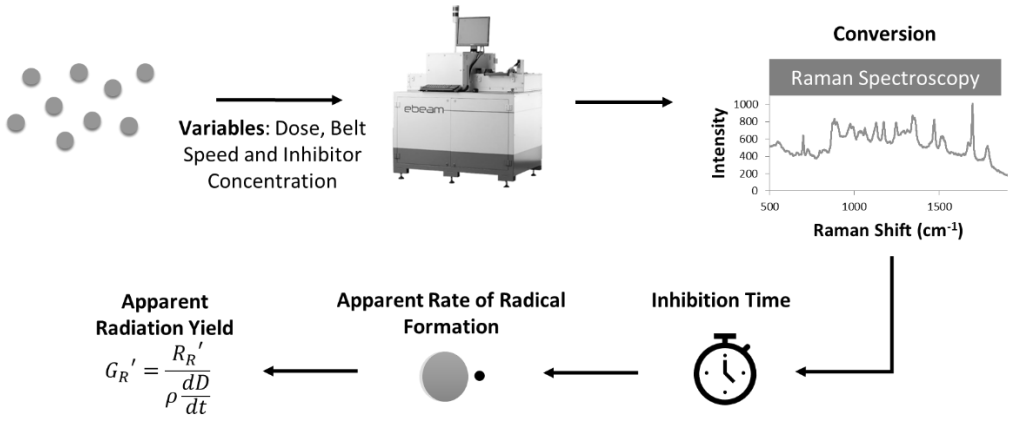

Figure 3. Overview of method used for determination of apparent radiation yield in EB polymerized samples.

To calculate conversion delay, a linear best-fit line was drawn through all points that were consistently above 5% conversion (polymerization regime). The cut-off at 5% conversion was chosen because the Raman spectrometer has an error of $\pm$ 5%. A second linear best-fit line was drawn through all points that were not consistently above 5% conversion (inhibition regime). The intersection of the two best-fit lines identified the conversion delay for the sample. The goodness of fit, reported in R^2 values, was above 0.9855 for the polymerization regime trendlines; however, the trendlines for the inhibition regime had significantly lower R^2 values, ranging between 0.058 and 0.9801. The low R^2 values can be attributed to the large amount of Raman error at low conversions. Because the conversion is not yet increasing, the large, random variation in Raman measurements drastically reduces the goodness of fit.

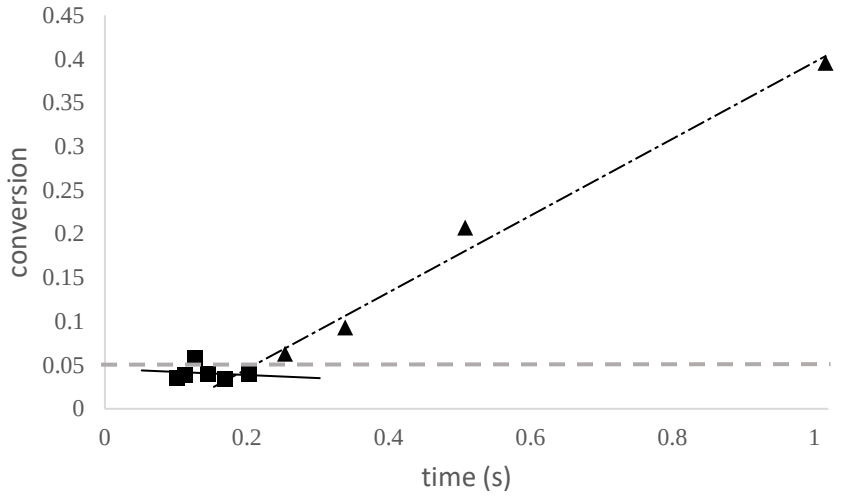

Figure 4. Representative kinetic profile resulting from piecing together dose-belt speed trials. The formulation presented contains 1.5wt% HQ inhibitor in BA. The trendline for the square data points covers the inhibition regime, and the trendline for the triangular data points spans the polymerization regime. Linear best fit lines were drawn through each regime, and the intersection was taken to be the conversion delay.

A conversion delay also occurs in the pure monomer sample, which does not contain any HQ. This delay stems from dissolved oxygen in the sample, which reacts with the free radicals to produce inactive peroxy radicals, as well as from the small amount of inhibitor added by the manufacturer to increase the shelf-life stability of the monomer. For this reason, the inherent inhibition delay observed in the neat BA sample was subtracted from the total conversion delay for each of the formulations containing inhibitor to obtain the inhibition time that was specifically due to the HQ inhibitor molecules (Equation 6).

$$inhibition\ time = conversion\ delay - inherent\ inhibition\ delay \quad (6)$$

These inhibition times were then plotted with respect to the inhibitor concentration, and a linear best-fit line was drawn (see Figure 5 as an example). The slope of the resulting trendline represents the change in inhibitor concentration with respect to time. Since it is assumed that each inhibitor molecule reacts with one radical, this value is equivalent to the change in radical

concentration with respect to time, which is equivalent to the apparent rate of radical formation, R_R' (Equation 7).

$$\frac{d[inhibitor]}{dt} = \frac{d[R*]}{dt} = {R_R}' \tag{7}$$

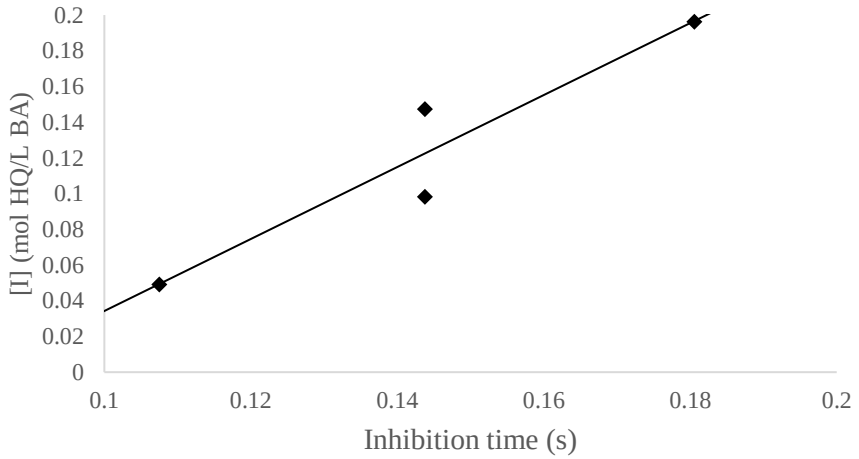

Figure 5. Representative profile used to determine the apparent rate of radical formation, R_R'. The slope of the resulting best-fit line was equal to R_R'; the goodness of fit, reported as R^2 values, was above 0.7449 for all three trials of BA formulations containing HQ inhibitor.

Using the calculated value for R_R', the known density of BA, and set dose rate, the apparent radiation was calculated using Equation 3. A sample calculation of apparent radiation yield is shown below:

$$G'_R = \frac{0.9664\ mol\ L^{-1}s^{-1}}{1.06\ g\ mL^{-1}(196.8\ J\ g^{-1}s^{-1})} \times \frac{J}{2.242 \times 10^{18} eV} \times \frac{L}{1000 mL} \times \frac{6.022 \times 10^{23}}{mol} \times 100 eV$$

In this calculation, several unit conversions must be completed so that the results are reported in number of initiating radicals created per 100 eV of energy absorbed by the system. These included conversions from J to eV, mL to L, and moles to radicals (using Avogadro's number). Finally, the result was multiplied by 100 eV to be consistent with the definition of apparent

radiation yield. The apparent radiation yield was calculated for three trials, and the results are given in Table 2.

Table 2. Apparent radiation yield (G_R') for BA

	Trial 1	**Trial 2**	**Trial 3**	**Average**
G_R'	30	45	99	60±40

Discussion

The apparent radiation yield of BA was calculated to be 60±40 using the newly developed protocol. This average is based on three trials and had a large standard deviation. However, the values obtained are physically reasonable. G_R' is defined per 100 eV of energy absorbed by the system. Based on the bond dissociation energies of C-H bonds, it takes roughly 3.5-4.5 eV of energy to break the bond, which creates two radicals. The exact bond dissociation energy depends on the groups adjacent to the C-H bond. Selected examples of bond dissociation energies are given in Table 3.

Table 3. Select common bond dissociation energies for C-H bonds.

Bond	**Dissociation Energy (eV)**
H-CH_2CH_3	4.25
H-$CH_2CH_2CH_3$	4.25
H-$COCH_2CH_3$	3.78

Assuming a dissociation energy of 3.78 eV, the maximum number of radicals that 100 eV of energy can produce can be calculated as follows:

$$\frac{100\ eV\ absorbed}{3.78\ eV/bond} \times 2\frac{radicals}{bond} = 52.91\ radicals$$

The calculation shows the theoretical maximum number of radicals that can be produced by 100 eV of energy is just under 53.

In comparison to this maximum theoretical value of radicals, the mean G_R' value of 60±40 calculated seems reasonable. This value is within the same order of magnitude of the maximum amount that can be formed. It is expected that the G_R' value would be lower than the maximum number of radicals produced, as not all radicals that are produced can be measured. There is confidence that the values obtained are in the right range, but further work must be completed to reduce the standard deviation of the measurements. One major reason for the large standard deviation is due to the error in Raman measurements. Each measurement has a ~5% error associated with it, and this error continues to propagate through the analysis because those measurements are used to determine inhibition times and to create plots from which the slope is used to obtain the apparent rate of radical formation. Small errors in initial measurements can quickly result in large deviations in the final value. Future work will focus on reduction of these errors in the conversion measurements.

Error in the values for apparent radiation yield can be reduced by using an alternative method to obtain the apparent rate of radical formation of each sample. Use of a different inhibitor (DPPH), which is colored, allows the disappearance of inhibitor to be directly monitored using a UV-Vis spectrophotometer. As the reaction progresses, a color change occurs, and the amount of color change in the sample signifies the amount of inhibitor that has reacted. From this analysis, change in inhibitor concentration with respect to time is directly obtained, and therefore apparent rate of radical formation can also be directly obtained. Because this method directly measures the apparent rate of radical formation, the data analysis is simplified, and the error is greatly reduced.

Another reason for the large standard deviation is that EB is random. Radicals interact with the monomer and polymer samples and can lead to many different complex reactions. These radicals can go on to propagate and form long chain polymers, cross-links between polymer chains, or react in many other ways. The exact reactions that take place are different every time, and as such, the number of measurable radicals created may vary significantly each time.

Conclusions

A promising protocol was developed to determine the apparent radiation yield of EB-polymerized samples. The resulting values were physically reasonable, with an average value of 60±40. Future work will focus on reduction of error in the sample measurements. Once error has been effectively reduced, the apparent radiation yield of other monomers will be compared.

Acknowledgements

This project was supported by the National Science Foundation under Grant No. 1264622 and the Iowa Center for Research by Undergraduates. The author would like to acknowledge Nicole Kloepfer and Dr. Julie Jessop for their guidance throughout this project. The author would also like to acknowledge eT for use of their EB equipment.

References

Allen, C. C., Oraby, W., Hossain, T. M., Stahel, E. P., Squire, D. R., & Stannett, V. T. (1974). Studies in Radiation-Induced Polymerization of Vinyl Monomers at High Dose-Rates. II. Methyl Methacrylate. *Journal of Applied Polymer Science, 18*, 709-725.

Chapiro, A. (1962). *Radiation Chemistry of Polymeric Systems.* New York : John Wiley & Sons.

Labana, S. S. (1968). Kinetics of High-Intensity Electron-Beam Polymerization of a Divinyl Urethane. *Journal of Polymer Science: Part A-1, 6*, 3283-3293.

Schissel, S. M., Lapin, S. C., & Jessop, J. L. (2014). Internal reference validation for EB-cured polymer conversions measured via Raman spectroscopy. *RadTech Rep.*, 46-50.

Squire, D. R., Cleaveland, J. A., Hossain, T. M., Oraby, W., Stahel, E. P., & Stannett, V. T. (1972). Studies in Radiation-Induced Polymerization of Vinyl Monomers at High Dose Rates. I. Styrene. *Journal of Applied Polymer Science, 16*, 645-661.

Appendices

Contents

Appendix A: Graphs of conversion versus time for each concentration of inhibitor

The following figures were used in the data analysis for this research. These contain representative kinetic profiles resulting from piecing together dose-belt speed trials. The formulations presented contain differing amounts of HQ inhibitor in BA, which is signified in the subheadings. The trendline for the square data points covers the inhibition regime, and the trendline for the triangular data points spans the polymerization regime. Linear best fit lines were drawn through each regime, and the intersection was taken to be the conversion delay.

Neat BA

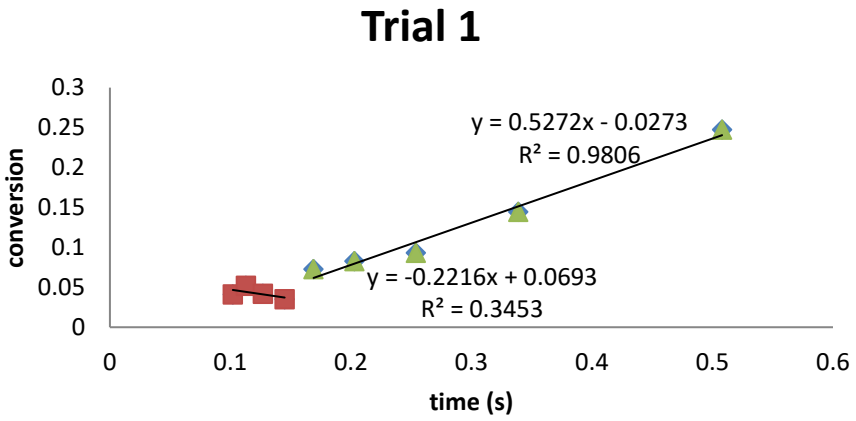
Trial 1
conversion
time (s)
y = 0.5272x - 0.0273
R² = 0.9806
y = -0.2216x + 0.0693
R² = 0.3453
0.3
0.25
0.2
0.15
0.1
0.05
0
0
0.1
0.2
0.3
0.4
0.5
0.6

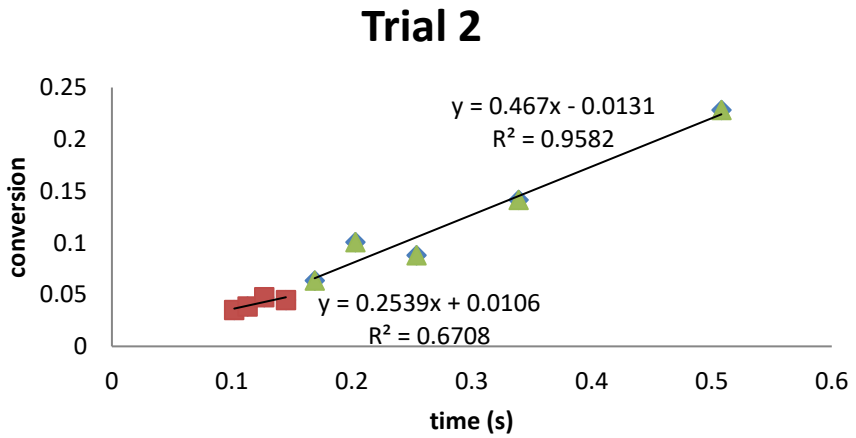
Trial 2
conversion
time (s)
y = 0.467x - 0.0131
R² = 0.9582
y = 0.2539x + 0.0106
R² = 0.6708
0.25
0.2
0.15
0.1
0.05
0
0
0.1
0.2
0.3
0.4
0.5
0.6

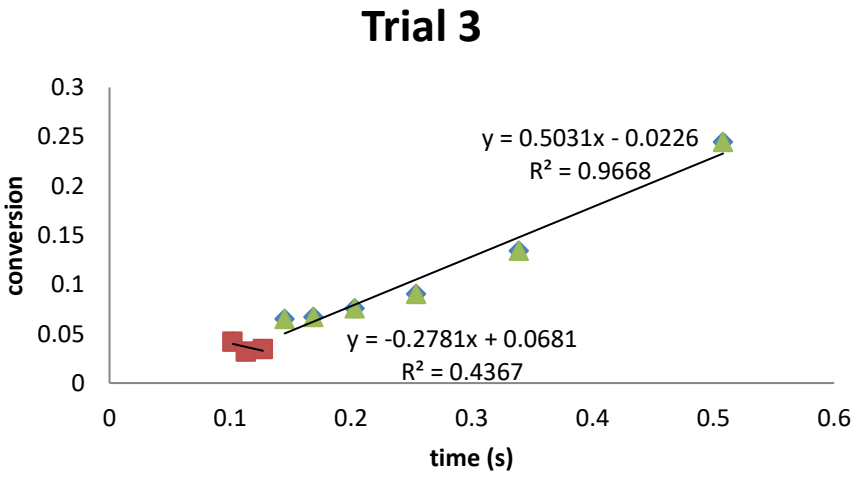
Trial 3
conversion
time (s)
y = 0.5031x - 0.0226
R² = 0.9668
y = -0.2781x + 0.0681
R² = 0.4367
0.3
0.25
0.2
0.15
0.1
0.05
0
0
0.1
0.2
0.3
0.4
0.5
0.6

0.25% HQ

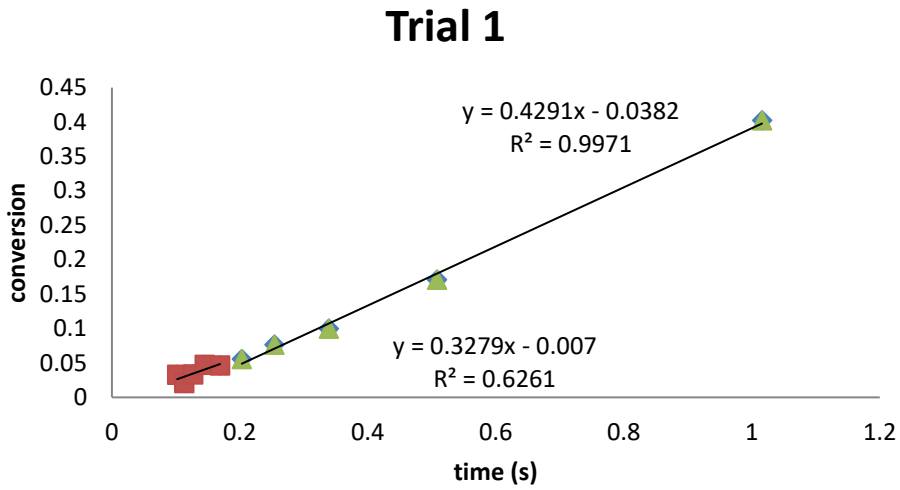
Trial 1
y = 0.4291x - 0.0382
R² = 0.9971
y = 0.3279x - 0.007
R² = 0.6261
conversion
time (s)
0.45
0.4
0.35
0.3
0.25
0.2
0.15
0.1
0.05
0
0
0.2
0.4
0.6
0.8
1
1.2

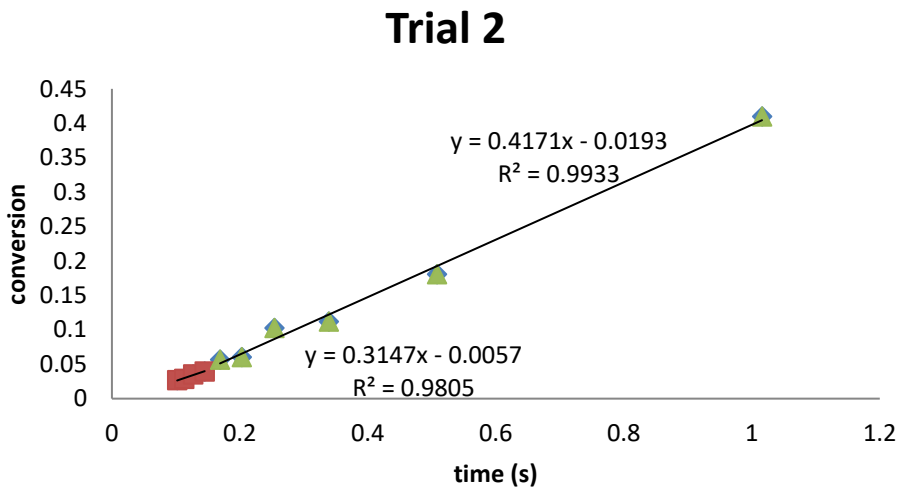
Trial 2
y = 0.4171x - 0.0193
R² = 0.9933
y = 0.3147x - 0.0057
R² = 0.9805
conversion
time (s)
0.45
0.4
0.35
0.3
0.25
0.2
0.15
0.1
0.05
0
0
0.2
0.4
0.6
0.8
1
1.2

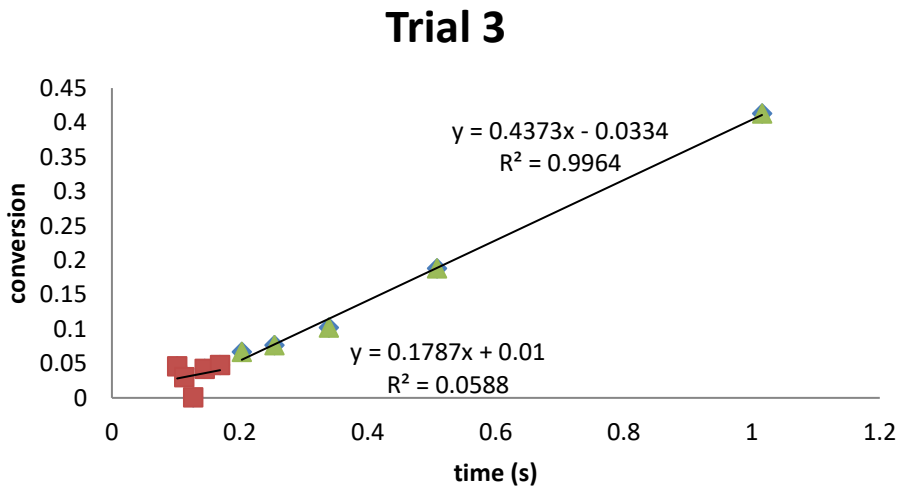
Trial 3
y = 0.4373x - 0.0334
R² = 0.9964
y = 0.1787x + 0.01
R² = 0.0588
conversion
time (s)
0.45
0.4
0.35
0.3
0.25
0.2
0.15
0.1
0.05
0
0
0.2
0.4
0.6
0.8
1
1.2

0.5% HQ

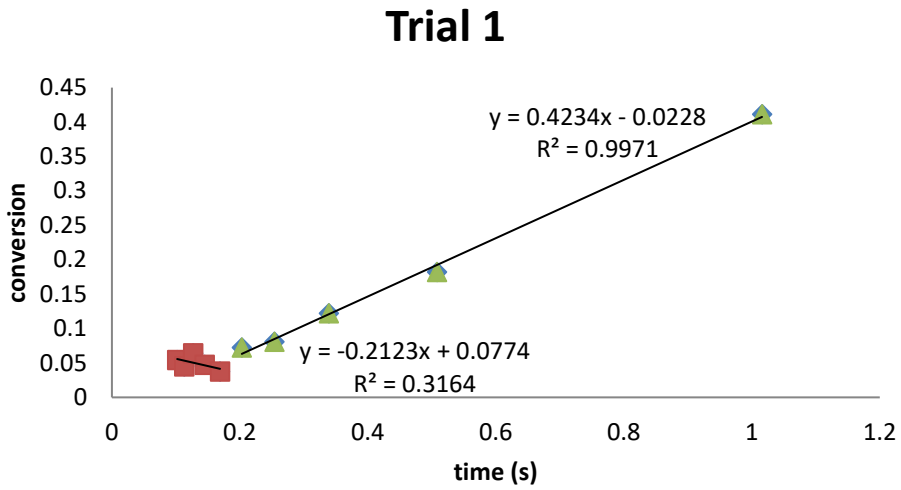
Trial 1
y = 0.4234x - 0.0228
R² = 0.9971
y = -0.2123x + 0.0774
R² = 0.3164
conversion
time (s)
0.45
0.4
0.35
0.3
0.25
0.2
0.15
0.1
0.05
0
0
0.2
0.4
0.6
0.8
1
1.2

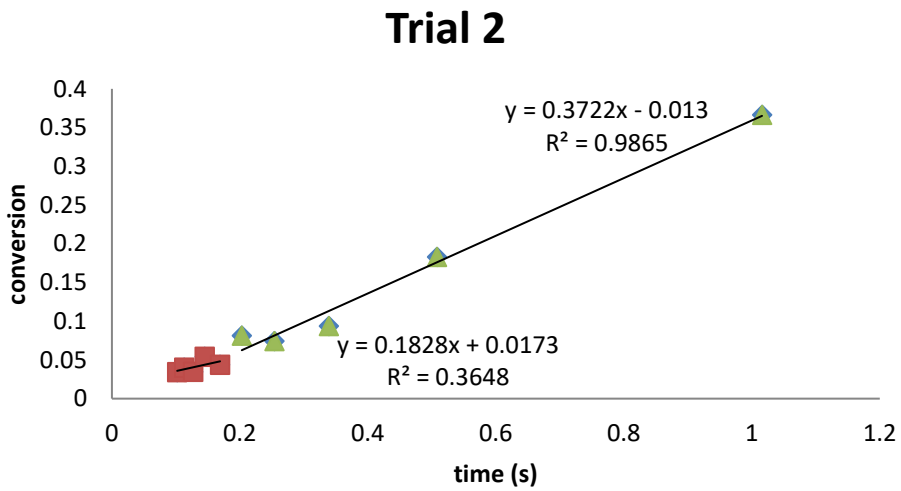
Trial 2
y = 0.3722x - 0.013
R² = 0.9865
y = 0.1828x + 0.0173
R² = 0.3648
conversion
time (s)
0.4
0.35
0.3
0.25
0.2
0.15
0.1
0.05
0
0
0.2
0.4
0.6
0.8
1
1.2

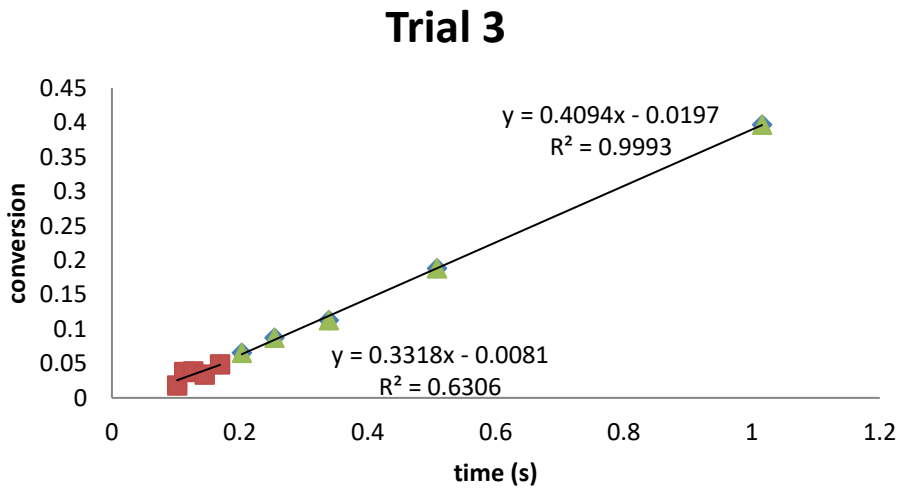
Trial 3
y = 0.4094x - 0.0197
R² = 0.9993
y = 0.3318x - 0.0081
R² = 0.6306
conversion
time (s)
0.45
0.4
0.35
0.3
0.25
0.2
0.15
0.1
0.05
0
0
0.2
0.4
0.6
0.8
1
1.2

1% HQ

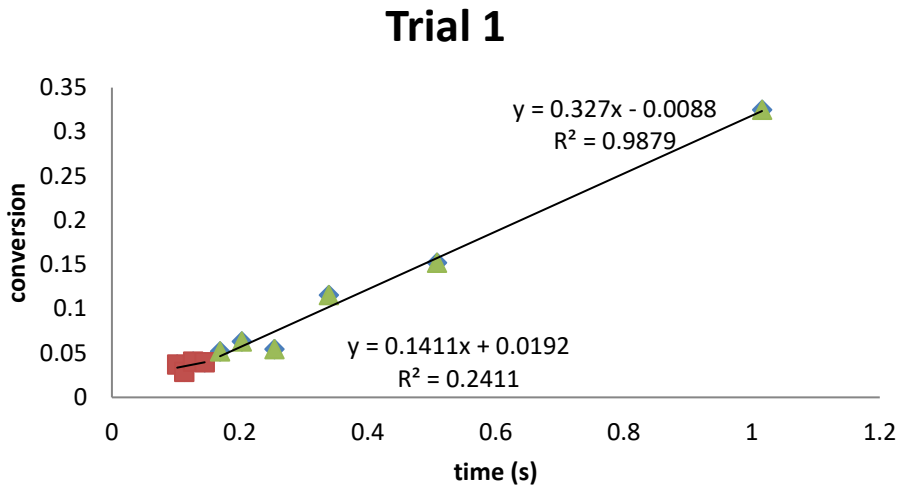
Trial 1
y = 0.327x - 0.0088
R² = 0.9879
y = 0.1411x + 0.0192
R² = 0.2411
conversion
time (s)
0
0.05
0.1
0.15
0.2
0.25
0.3
0.35
0.2
0.4
0.6
0.8
1
1.2

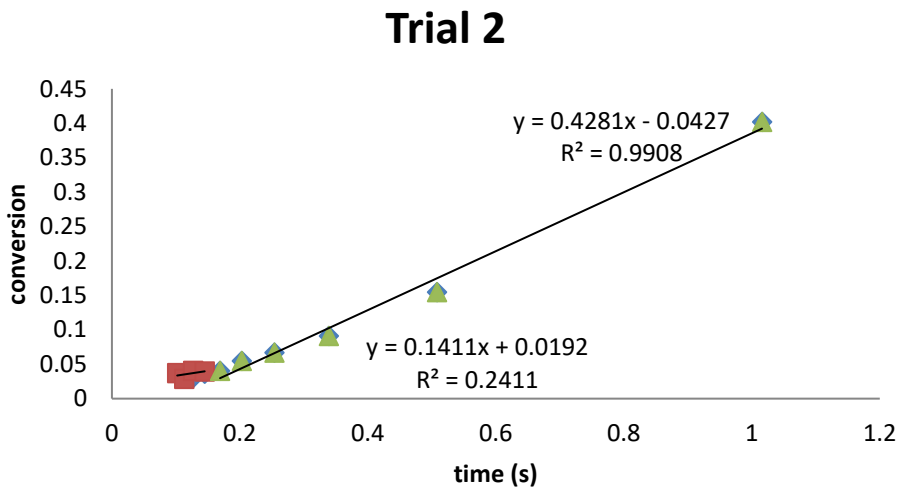
Trial 2
y = 0.4281x - 0.0427
R² = 0.9908
y = 0.1411x + 0.0192
R² = 0.2411
conversion
time (s)
0
0.05
0.1
0.15
0.2
0.25
0.3
0.35
0.4
0.45
0.2
0.4
0.6
0.8
1
1.2

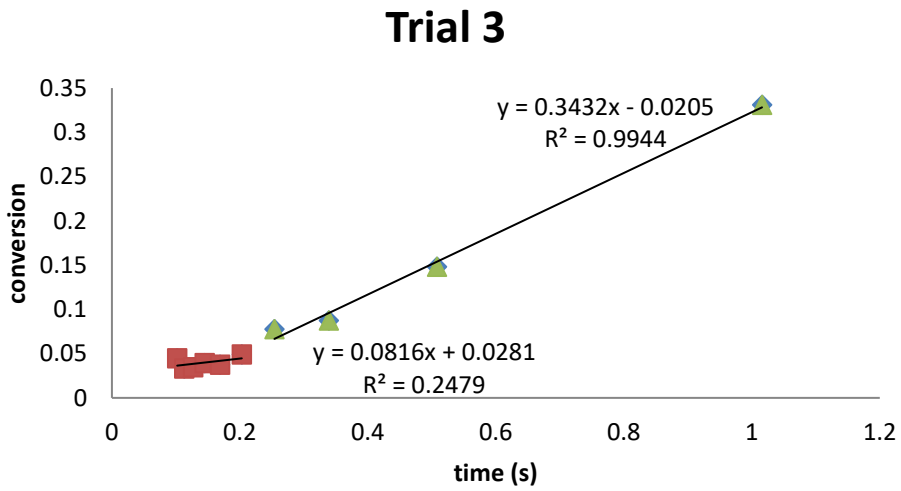
Trial 3
y = 0.3432x - 0.0205
R² = 0.9944
y = 0.0816x + 0.0281
R² = 0.2479
conversion
time (s)
0
0.05
0.1
0.15
0.2
0.25
0.3
0.35
0.2
0.4
0.6
0.8
1
1.2

1.5% HQ

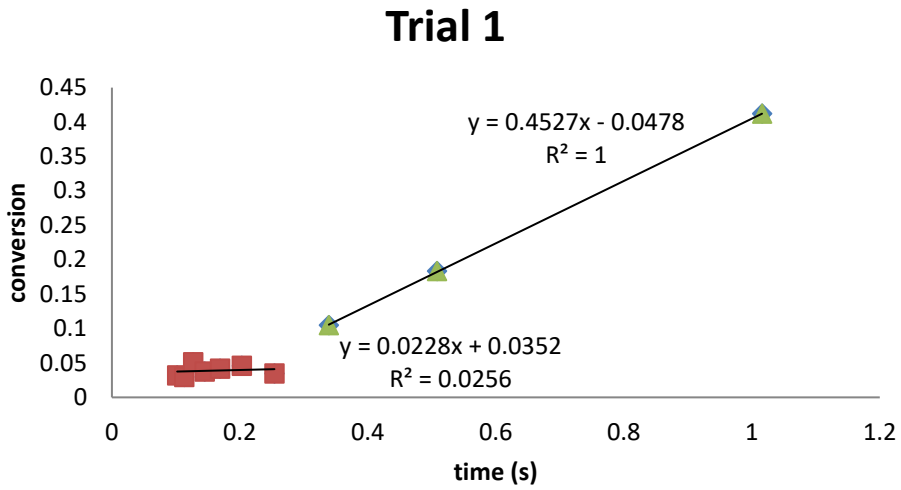
Trial 1
y = 0.4527x - 0.0478
R² = 1
y = 0.0228x + 0.0352
R² = 0.0256
conversion
time (s)
0.45
0.4
0.35
0.3
0.25
0.2
0.15
0.1
0.05
0
0
0.2
0.4
0.6
0.8
1
1.2

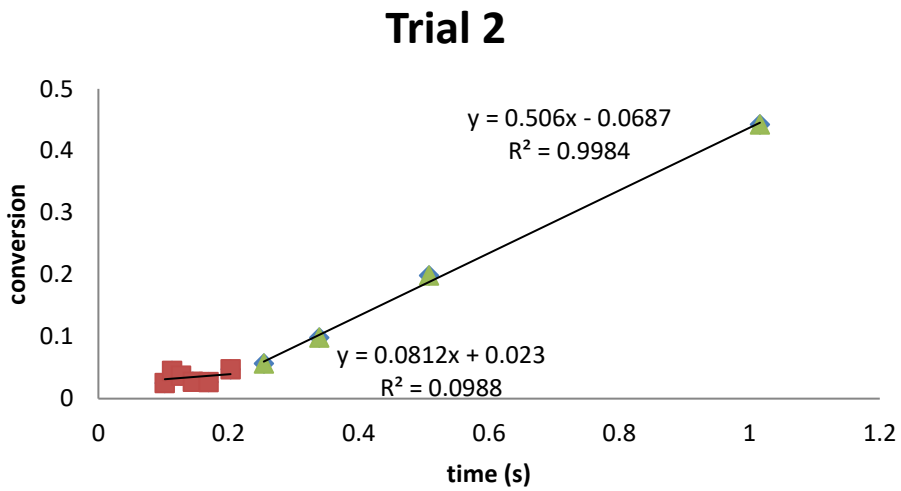
Trial 2
y = 0.506x - 0.0687
R² = 0.9984
y = 0.0812x + 0.023
R² = 0.0988
conversion
time (s)
0.5
0.4
0.3
0.2
0.1
0
0
0.2
0.4
0.6
0.8
1
1.2

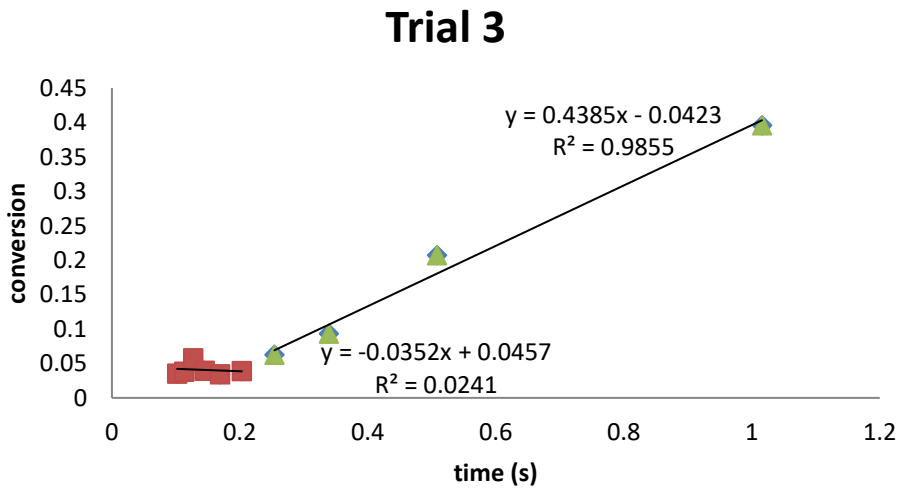
Trial 3
y = 0.4385x - 0.0423
R² = 0.9855
y = -0.0352x + 0.0457
R² = 0.0241
conversion
time (s)
0.45
0.4
0.35
0.3
0.25
0.2
0.15
0.1
0.05
0
0
0.2
0.4
0.6
0.8
1
1.2

2% HQ

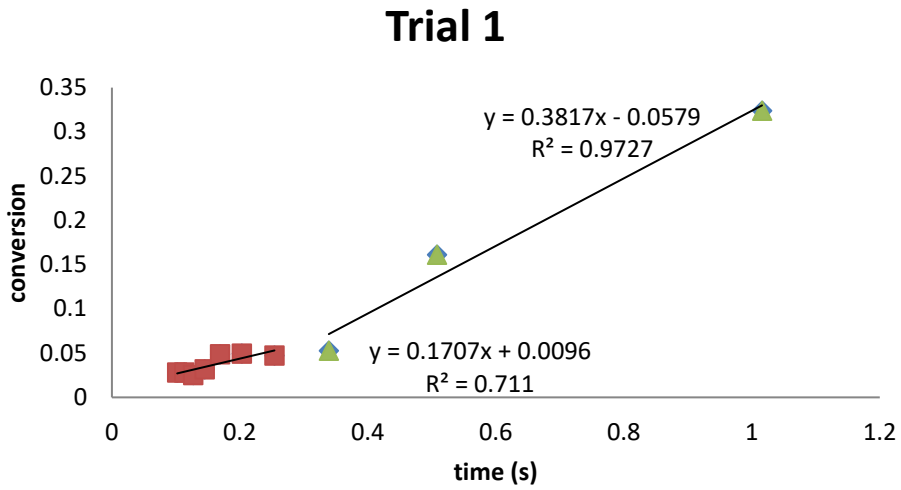
Trial 1
y = 0.3817x - 0.0579
R² = 0.9727
y = 0.1707x + 0.0096
R² = 0.711
conversion
time (s)
0.35
0.3
0.25
0.2
0.15
0.1
0.05
0
0
0.2
0.4
0.6
0.8
1
1.2

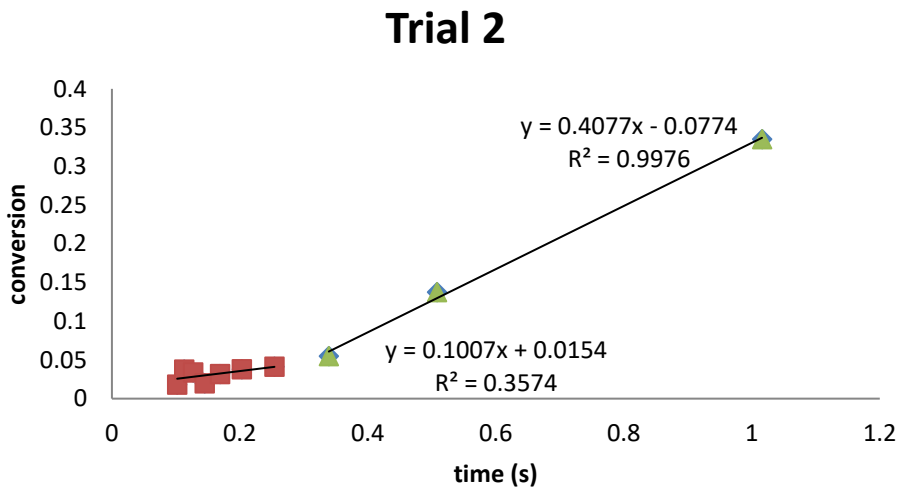
Trial 2
y = 0.4077x - 0.0774
R² = 0.9976
y = 0.1007x + 0.0154
R² = 0.3574
conversion
time (s)
0.4
0.35
0.3
0.25
0.2
0.15
0.1
0.05
0
0
0.2
0.4
0.6
0.8
1
1.2

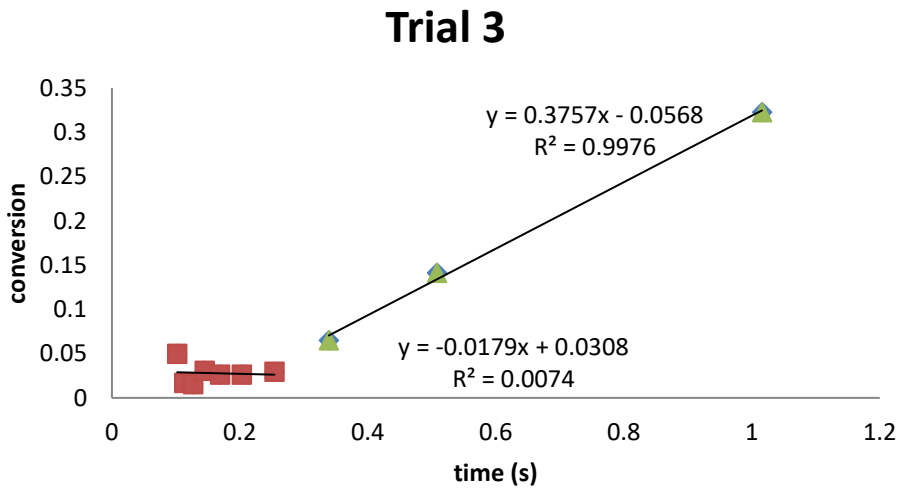
Trial 3
y = 0.3757x - 0.0568
R² = 0.9976
y = -0.0179x + 0.0308
R² = 0.0074
conversion
time (s)
0.35
0.3
0.25
0.2
0.15
0.1
0.05
0
0
0.2
0.4
0.6
0.8
1
1.2

Appendix B: Graphs of inhibitor concentration versus inhibition time

The following figures are the profiles for the three trials used to determine the apparent rate of radical formation, R_R'. The slope of the resulting best-fit line was equal to R_R'.

Trial 1

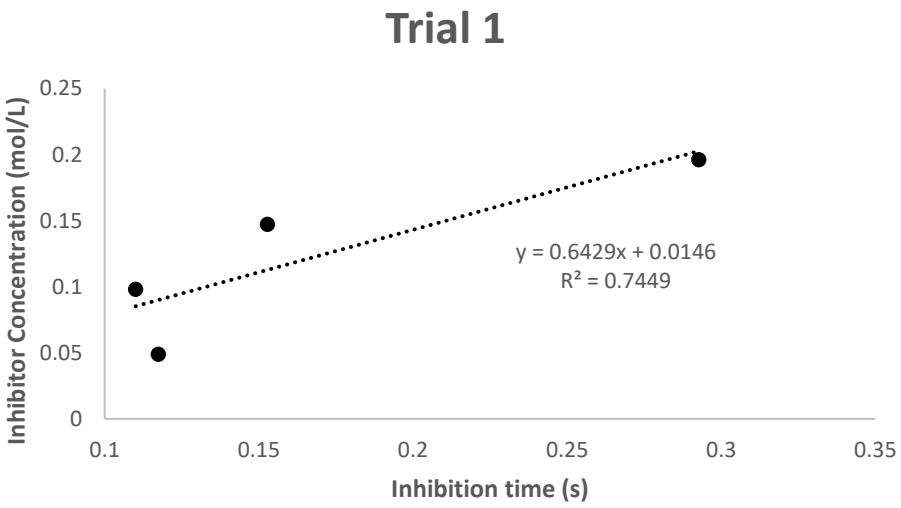

Trial 2

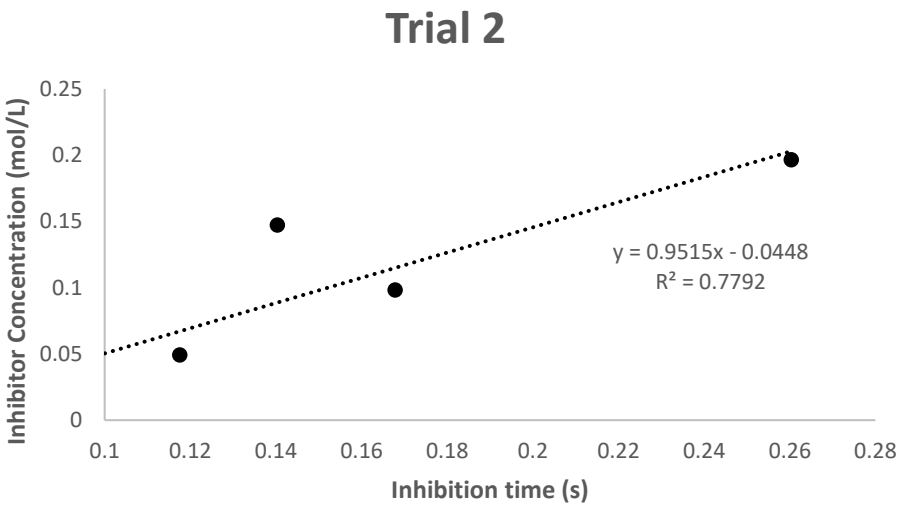

Trial 3

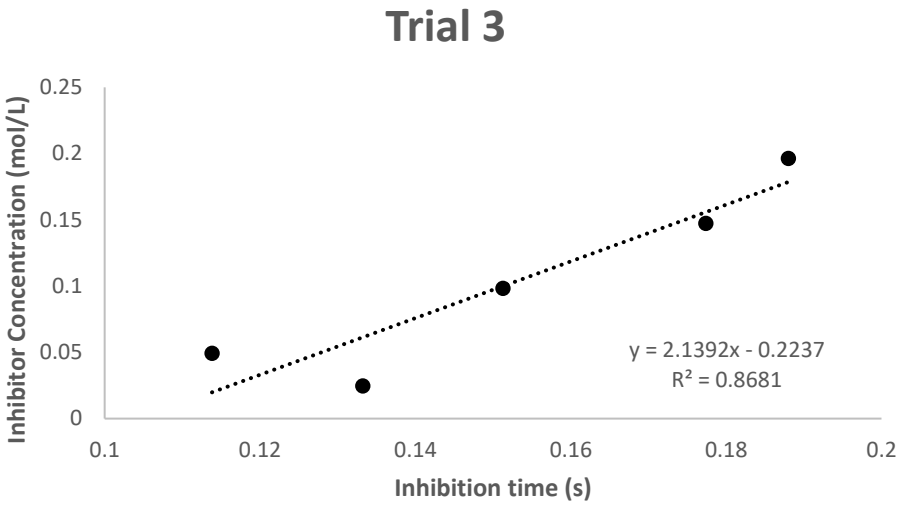
Trial 3
Inhibitor Concentration (mol/L)
0.25
0.2
0.15
0.1
0.05
0
0.1
0.12
0.14
0.16
0.18
0.2
Inhibition time (s)
y = 2.1392x - 0.2237
R² = 0.8681